



Invited Article

Dynamics and control of molten-salt breeder reactor

Vikram Singh^{*}, Matthew R. Lish, Ondřej Chvála, Belle R. Upadhyaya

Department of Nuclear Engineering, 315 Pasqua Engineering Building, University of Tennessee, Knoxville, TN 37996, USA

ARTICLE INFO

Article history:

Received 30 May 2017

Received in revised form

19 June 2017

Accepted 19 June 2017

Available online 26 June 2017

Keywords:

MSBR

molten-salt

two-fluid

dynamic analysis

control

load-following

thorium

ABSTRACT

Preliminary results of the dynamic analysis of a two-fluid molten-salt breeder reactor (MSBR) system are presented. Based on an earlier work on the preliminary dynamic model of the concept, the model presented here is nonlinear and has been revised to accurately reflect the design exemplified in ORNL-4528. A brief overview of the model followed by results from simulations performed to validate the model is presented. Simulations illustrate stable behavior of the reactor dynamics and temperature feedback effects to reactivity excursions. Stable and smooth changes at various nodal temperatures are also observed. Control strategies for molten-salt reactor operation are discussed, followed by an illustration of the open-loop load-following capability of the molten-salt breeder reactor system. It is observed that the molten-salt breeder reactor system exhibits “self-regulating” behavior, minimizing the need for external controller action for load-following maneuvers.

© 2017 Korean Nuclear Society, Published by Elsevier Korea LLC. This is an open access article under the CC BY-NC-ND license (<http://creativecommons.org/licenses/by-nc-nd/4.0/>).

1. Introduction

The Molten-Salt Reactor Program (MSRP) operated from 1958 to 1976 at Oak Ridge National Laboratory (ORNL; 1 Bethel Valley Rd, Oak Ridge, TN 37830, USA) with the objective of developing fluid-fueled nuclear reactors that used solutions of fissile or fertile material in suitable carrier salts [1]. MSRP was preceded by the Aircraft Nuclear Propulsion (ANP) program during which the first molten-salt reactor (MSR), the Aircraft Reactor Experiment, was operated at ORNL in 1954. The experiment demonstrated desirable load-following features of the system, specifically the ability to drive the reactor power by heat demand alone [2].

A major achievement of the MSRP was the design, construction, and operation of the Molten-Salt Reactor Experiment (MSRE) between 1965 and 1969 [3]. Experiments carried out at the MSRE showed the practicality of handling molten salts in an operating reactor. The reactor's dynamic behavior correlated well with predictions. Many instruments were installed for reactor characterization, and control was mainly accomplished using more than 1,000 type-K thermocouples that measured temperature in various flow regions of the reactor system [4]. The MSRE is the only well-characterized operated MSR; therefore, its results serve as benchmarks for current MSR studies. Prior to the program's conclusion,

efforts were devoted to technology development needed for full-scale MSR demonstrations. Results from these studies are documented in hundreds of reports and peer-reviewed publications. A world-wide web repository of many of these documents can be found in Ref. [5].

The focus of this paper is to develop dynamic models and control strategies for a molten-salt breeder reactor (MSBR). This research and development is inspired by the work done by MSRP on a conceptual two-fluid breeder reactor [6]. A schematic is shown in Fig. 1. The modular design consists of four reactor modules with an electrical output of 250 MW/module. The two-fluid reactor has a graphite-moderated core with FLiBe salt circulated through the core and blanket containing UF₄ and ThF₄, respectively. Thorium in the blanket salt cannot directly undergo fission, but is converted into uranium-233 in a breeding process in which thorium absorbs a neutron and subsequently undergoes two beta decays, becoming U-233, which is fissile. Thorium is called a fertile species for its property of being converted to a fissile species after absorption of a neutron. The U-233 isotope is then separated from the blanket salt and introduced to the fuel salt to undergo fission in the reactor core. These reactors are also called liquid fluoride thorium reactors or LFTR, to emphasize their thorium/uranium fuel cycle as distinct from other MSR concepts.

The developed nonlinear nodal model accurately reflects the reactor design presented in the study by Robertson et al. [6] and simulates the dynamic behavior of neutron kinetics, heat transfer,

^{*} Corresponding author.

E-mail address: vsingh10@vols.utk.edu (V. Singh).

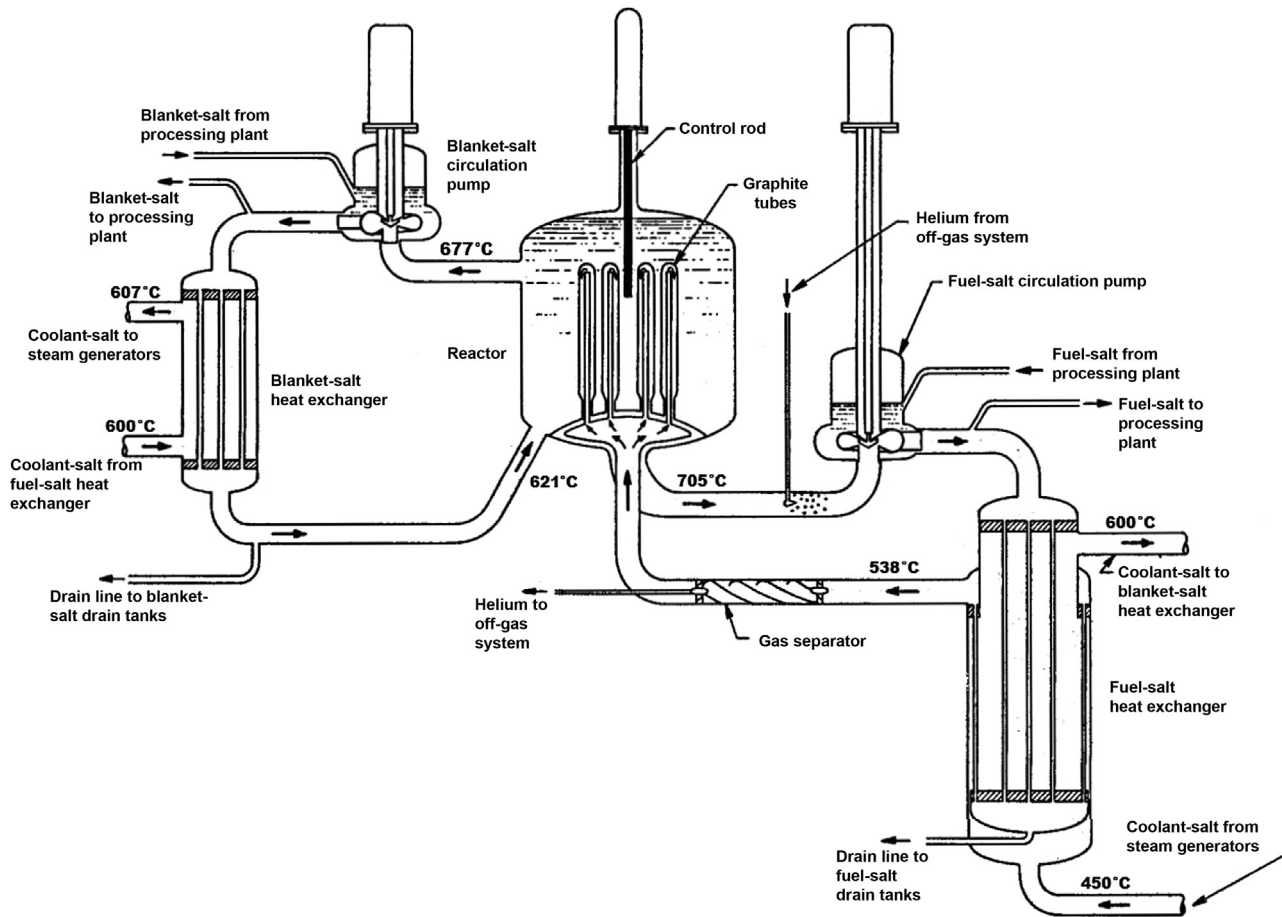


Fig. 1. Simplified schematic of the molten-salt breeder reactor system. (Source: ORNL-4528, Oak Ridge National Laboratory, 1970.)

and fluid transport in the MSBR. A detailed discussion of the model and its dynamics are presented in a companion paper. As noted earlier, MSRE results are the only benchmark for such models. Hence, a model extending the approach has been developed for the MSRE, and the results and comparisons are the topics of a companion paper under preparation.

This paper focuses on the basic dynamics of the uncontrolled MSBR and explores strategies for controlling the reactor system to improve upon uncontrolled performance. A major objective here is to study the controllability of the MSBR system based on model predictions and examine the need for control action. The open-loop load-following capability of the MSBR system is also demonstrated and its implications are discussed.

2. Description of the two-fluid reactor

The two-fluid MSBR was conceived at ORNL following the successful operation of the MSRE [6]. The design particularly seeks to utilize the thermal-spectrum Th–U233 breeding cycle while producing high-potential heat.

The two-fluid MSBR is a 1,000-MWe plant with four power-producing reactor modules of 556 MWth each. Each core module has a hexagonal lattice of graphite assemblies for neutron moderation. The graphite assembly design consists of a cylindrical sleeve surrounding a bore drilled in the center. This creates a hollow space for fuel salt to flow through the graphite matrix, while also separating the fissile and fertile material. UF_4 dissolved in ${}^7\text{LiF}\text{-BeF}_2$

(>99% enriched) is used as a fuel salt with the same molar and isotopic composition as given in the study by Robertson et al. [6].

The fuel salt circulated through the core enters at $\sim 537^\circ\text{C}$ through a lower plenum and flows up the graphite channels through the hollow cylindrical sleeves. It then flows down through the bores. Meanwhile, fissions occur in the salt during transit, and it leaves the core at the bottom of the reactor vessel at $\sim 705^\circ\text{C}$. The fuel salt then enters a countercurrent heat exchanger where heat energy is transferred to a secondary coolant salt.

The second of the two fluids, the fertile blanket salt, enters the reactor vessel at the bottom. The salt flows up both through interstitial spaces in the graphite channel matrix and in the blanket-only cells surrounding the core. This exposes the fertile material to higher neutron flux and encourages breeding. As a result, its temperature rises by $\sim 50^\circ\text{C}$. The blanket salt then flows through its own heat exchanger. The coolant salt leaving the fuel salt heat exchanger is pumped through the blanket salt heat exchanger in series. The coolant salt at $\sim 607^\circ\text{C}$ then flows into a conventional steam generator system and produces superheated steam.

Helium is used as the cover gas over the salt in the pump bowl and as the medium for stripping gaseous fission products from the salt. In the latter case, small bubbles of helium are injected into the salt in the suction line to the pump. The small quantities of xenon and other gases form nucleate with the helium bubbles. The helium is then removed with its burden of krypton and xenon in a centrifugal separator in the line from the outlet of the heat

exchanger to the reactor vessel. This mechanism is illustrated in Fig. 1 at the core fuel salt outlet [7]. Furthermore, the fluid salts allow for continuous batch processing to remove fission products of interest. The reactor operates at atmospheric pressure with a mean core outlet temperature of ~705°C. Major changes in reactivity are made by changing the fuel salt composition, i.e., by adding small amounts of uranium fuel. Minor reactivity changes are made by moving control rods to maintain temperature and steady-state operation [6].

3. Dynamic behavior

The assumptions made in the model presented along with some salient features of note are listed here to aid the reader: (1) the model presented is inherently nonlinear; (2) spatial dependence of the neutron flux is neglected; (3) all the power is assumed to be generated in the moderated region of the core; (4) there is no axial heat transfer between the moderated region of the core; (5) all fluid nodes are assumed to be well mixed; (6) the boiler/reheater system is not modeled; and (7) fission product removal is not modeled.

The modeling approach is to describe the dynamics of neutron density (reactor power), core heat transfer, fuel salt heat exchanger, and the blanket salt heat exchanger through nodalization. The “core” here refers only to the moderated region. The MSBR model described in this paper is based on an earlier work on the preliminary linearized dynamic model of the MSBR concept [8]. Revisions have been made to the original model to more accurately

depict the reactor design presented in the study of Robertson et al. [6] and to fully account for the nonlinear nature of the problem. This includes an updated nodal model shown in Fig. 2, based on core geometry considerations to separate the graphite mass into various nodes based on which graphite surfaces are in contact with the fuel and fertile salts.

The neutron dynamics is based on a point kinetics model with six delayed neutron precursors. It accounts for delayed neutron losses in external loops through the heat exchangers. No spatial variations of neutron flux are considered in this model. The core heat transfer consists of eight solid graphite nodes, eight fuel nodes, and four fertile nodes. The under-moderated blanket region is modeled using one node. The fuel is modeled as flowing up and then down through the graphite fuel assembly. Axial heat transfer in the graphite nodes is ignored, as shown in Fig. 2. All corresponding state variables are described by ordinary differential equations with delay terms included as required. The fuel salt heat exchanger is modeled using 11 nodes, which include two heat exchanger tube metal nodes and a mixing node. The fertile salt heat exchanger is similarly modeled using five nodes, one of which is a tube metal node. The coolant salt inlet temperature is a function of the dynamics on the secondary (or steam) side and is not modeled. It can be held constant or independently perturbed, if necessary, as an external input. The fertile salt heat exchanger is modeled with five nodes. The steam generator and the secondary side dynamics are not included in the current model.

The neutron dynamics is described by Eqs. (1 and 2) where $n(t)$ is the neutron density, $C_i(t)$ is the i^{th} delayed neutron precursor

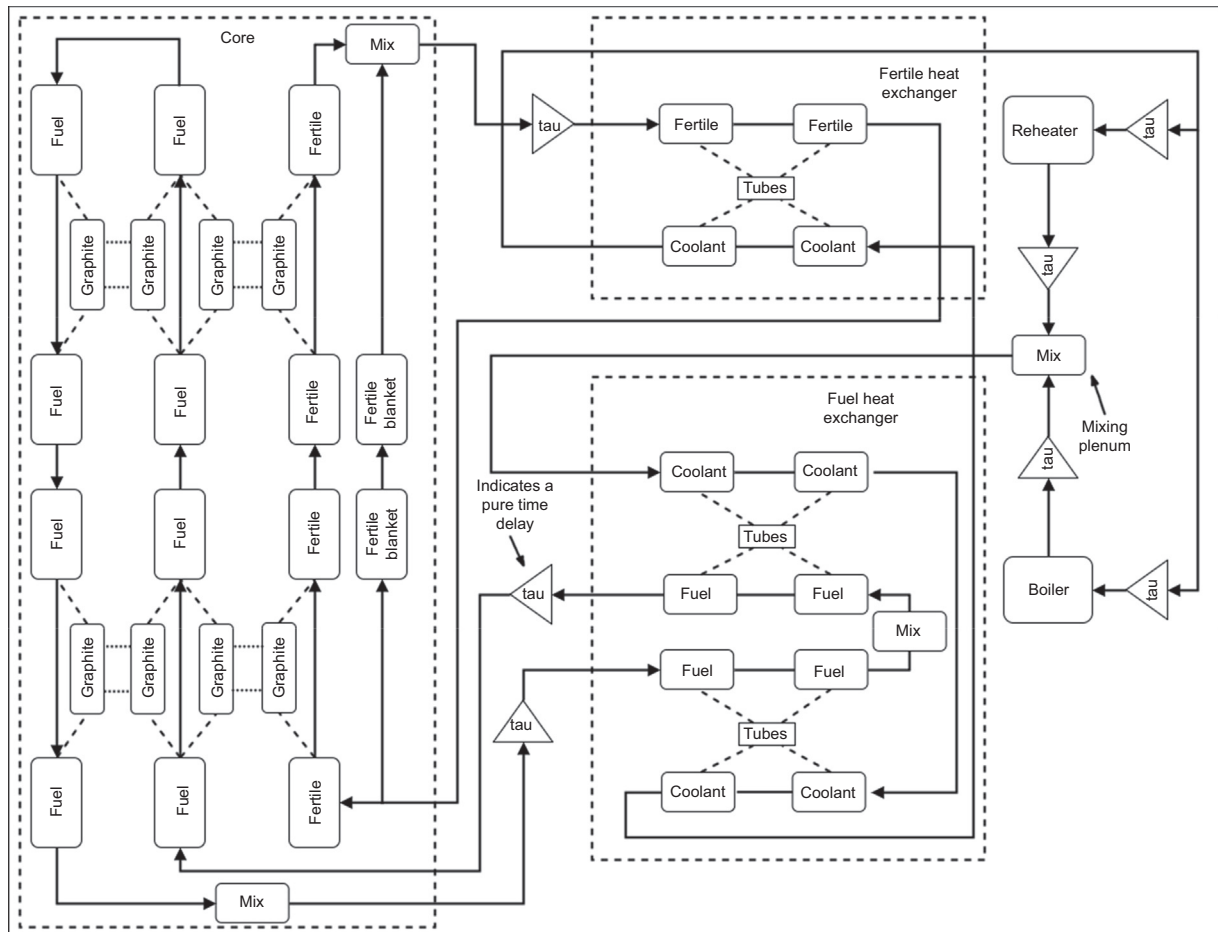


Fig. 2. Nodal model of the MSBR dynamics. Note that there is no axial heat transfer between the graphite nodes in the core. MSBR, molten-salt breeder reactor.

concentration (where $i = 1 \dots 6$), $\rho(t)$ is the total reactivity as a function of time (input), β_i is the delayed neutron fraction of the i^{th} delayed group, β is the total delayed neutron fraction, $S(t)$ is the source perturbation term, τ_c is the fuel transit time in the core (5.83 seconds), and τ_L is the fuel transit time in the external loop (9.25 seconds):

$$\frac{dn(t)}{dt} = \frac{(\rho(t) - \beta)}{\Lambda} n(t) + \sum_{i=1}^6 \lambda_i C_i(t) + S(t) \quad (1)$$

$$\frac{dC_i(t)}{dt} = \frac{\beta_i}{\Lambda} n(t) - \lambda_i C_i(t) + \frac{C_i(t - \tau_L) e^{-\lambda_i \tau_L}}{\tau_c} - \frac{C_i(t)}{\tau_c} \quad (2)$$

These are the modified point reactor kinetics equations, like those employed in the study of the MSRE [3]. They are nonlinear due to the product of reactivity and neutron density. Eq. (2) is a set of six equations for each of the delayed neutron precursor groups. The circulating fuel has the effect of reducing the effective delayed-neutron fraction and the rate of fuel temperature change during power changes. It also introduces delayed fuel temperature feedback and neutron-production effects. Hence, Eq. (2) accounts for the loss of delayed neutrons due to fuel transit. This modification also makes these a system of delayed differential equations, as seen in the third term in Eq. (2).

The total reactivity for the system is expressed as follows:

$$\rho = \rho_o + \rho_{fb} + \rho_{ext} \quad (3)$$

The feedback reactivity ρ_{fb} is contributed by changes in fuel, blanket, and graphite temperatures. With the above modifications, the reactivity necessary for steady-state operation ρ_o is nonzero and obtained from Eqs. (1 and 2). It is given as follows:

$$\rho_o = \beta - \sum_{i=1}^6 \frac{\beta_i}{\left(1 + \frac{1}{\lambda_i \tau_c} [1 - e^{-\lambda_i \tau_L}]\right)} \quad (4)$$

This ρ_o term is the reactivity change due to circulating fuel and accounts for delayed neutrons lost in transit. The calculated value is $\rho_o \approx 0.0012659$.

Temperature change equations for the various nodes account for any power generation in the node and energy transfer between nodes. For example, a fuel node is modeled as the sum of power generated in the node and energy transferred to the node from other fuel and graphite nodes [Eq. (5)].

$$\frac{dT_{f1}}{dt} = \frac{W_f}{m_{f1}} (T_{fin} - T_{f1}) + \frac{K_{f1} P_0 \left(\frac{n}{n_0}\right)}{m_{f1} C_{pf1}} + \frac{K_1 h A_{fg}}{m_{f1} C_{pf1}} (T_{g1} - T_{f1}) \quad (5)$$

Here, W_f is the fuel mass flow rate, m_{f1} is the mass of fuel node 1, K_{f1} is the power generated in fuel node 1, $h A_{fg}$ is the product of area and heat transfer coefficient for the fuel–graphite interface, and the T 's represent the temperatures of the various nodes. Assuming that the heat capacity of the salts does not change considerably within the operating temperature range, the power generated in the salts is given simply by the product of the mass flow rate, specific heat capacity, and ΔT , the difference between the inlet and outlet temperatures of the salt.

The steady-state parameters, and hence the initial conditions of the model, are characterized by design temperature targets, which are adopted from the work of Robertson et al. [6]. Furthermore, all liquid nodes are assumed to be well mixed, that is, the temperature of the liquid exiting the node is the same as the temperature in the node. Similar heat transfer equations are constructed for every node in Fig. 2. The nodes are named as follows: fuel nodes— f_i ,

graphite nodes— g_i , and blanket nodes— b_i . The axial nodes are divided into regions “a” and “b” denoted by the subscripts. This naming scheme was used purely for convenience and any mention of the nodes is accompanied by a brief description.

The model was developed in MATLAB–Simulink, using appropriate tools for solving nonlinear equations and for the graphical representation of the nodal model [9]. Some physical parameters of interest for the MSBR system are listed in Table 1. It is emphasized that this is an open-loop model without any external control action. All power is assumed to be generated in the moderated region only. Power generated in the fuel during external transit due to decay and gamma heating is ignored. Only the salt side of the final boiler/reheater heat sink is modeled. Heat removed by the steam generator and reheater is approximated by constant removal terms, which can be perturbed as external inputs.

Reactor responses to standard reactivity perturbations are presented. Fig. 3 shows a plot of the fractional power for an external reactivity step of 10^{-4} (10 pcm). Also shown is the feedback reactivity, resulting from step reactivity insertion. The power transient shows a prompt jump immediately following the step insertion.

This is followed by an exponential decrease due to the net negative temperature feedback effect. A rise (local peak) is seen after the initial transient in the otherwise smooth curve, due to delayed neutrons being brought back into the core by the circulating fuel. Upon closer examination, higher-order peaks are also seen in the exponential curve. There is also a rise in the feedback reactivity due to delayed changes in the core salt inlet temperatures following the reactivity perturbation. The duration of the peak corresponds approximately to the residence time of the fuel salt in the external loop, that is, τ_L (9.25 seconds).

The fractional power in the core returns to its nominal value after several minutes due to the constant power withdrawal terms in the final heat sink. The temperatures of the fuel and fertile nodes, however, acquire a higher steady-state value to compensate for the added reactivity. The negative feedback reactivity of the fuel thus allows for a lower steady-state ρ_{fb} as seen in Fig. 3B.

The stability of MSBR under periodic changes is studied by external stepwise reactivity perturbation of ± 60 pcm. Fig. 4 illustrates the response of fractional power and associated reactivity feedback, and demonstrates the stability of the MSBR system for large periodic reactivity excursions. The plot in Fig. 4B shows the natural feedback response of the reactor, which is essentially the inverse of the reactivity insertions. Similarly, other state variables such as fuel and graphite temperatures also respond to periodic perturbations in a stable fashion. Fig. 5A shows the temperatures of fuel upflow nodes with fuel salt entering at $f_2 b_2$, Fig. 5B temperatures of fuel downflow nodes with fuel salt exiting at node $f_1 b_1$, Fig. 5C temperatures of fuel to fuel graphite nodes, and Fig. 5D temperatures of fuel to fertile graphite nodes. It is also noted that a $\sim 15\%$ change in power is associated with a change in the fuel temperature difference, ΔT , of only about $\sim 10^\circ\text{C}$.

Table 1
Physical parameters for core components.

Parameter	Value in SI units
Fuel salt heat capacity C_{pf}	2.303×10^{-3} MJ/kg/ $^\circ\text{C}$
Graphite heat capacity C_{pg}	1.679×10^{-3} MJ/kg/ $^\circ\text{C}$
Fuel salt reactivity coefficient α_f	-8.172×10^{-5} $\rho/^\circ\text{C}$
Graphite reactivity coefficient α_g	2.016×10^{-5} $\rho/^\circ\text{C}$
Total delayed neutron fraction for U-233 β	0.002896
Neutron generation time Λ	3.3×10^{-4} sec
Fuel salt external loop time τ_L	9.25 sec
Fuel salt core transit time τ_c	5.83 sec
Fraction of power generated in fuel salt	0.884

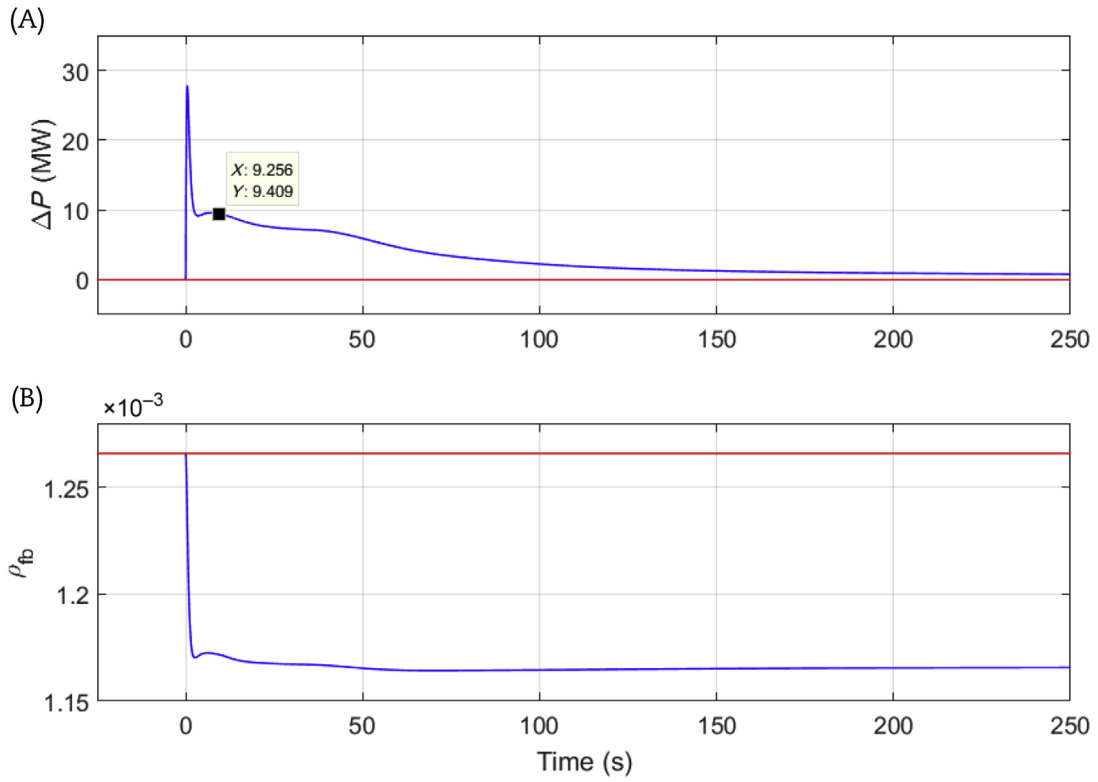


Fig. 3. Reactor response to standard reactivity perturbations. (A) Power and (B) feedback reactivity response to +10 pcm step insertion at nominal power of 556 MW(th). Steady-state values are shown in red.

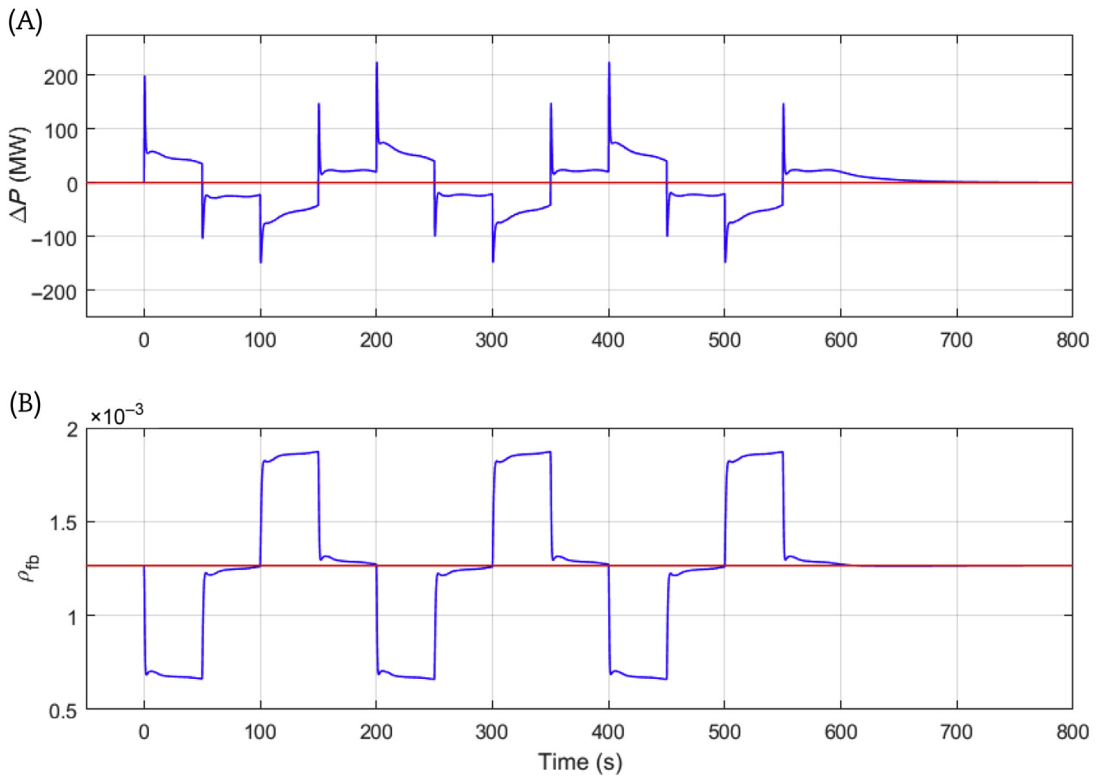


Fig. 4. Stability of MSBR under periodic changes. (A) Power and (B) feedback reactivity response to periodic reactivity of ± 60 pcm at nominal power of 556 MW(th). MSBR, molten-salt breeder reactor.

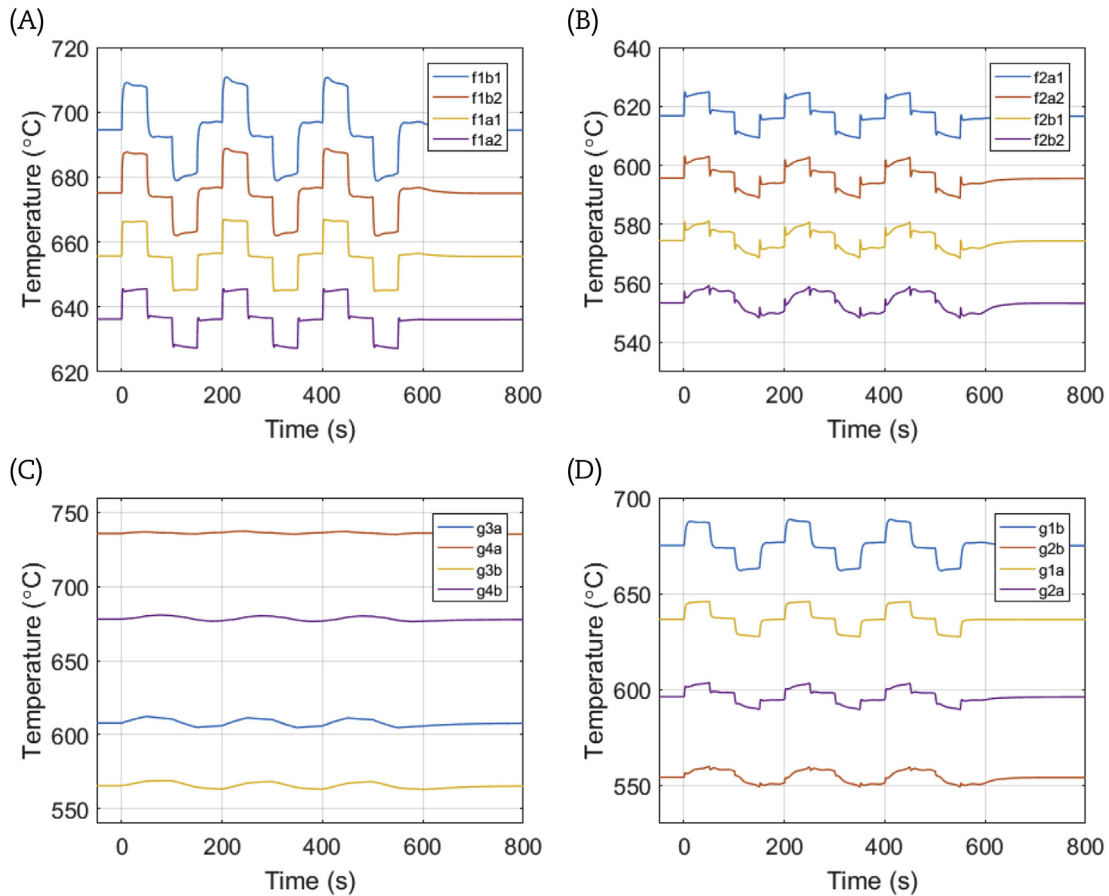


Fig. 5. Responses of fuel and graphite temperatures to periodic perturbations. Nodal temperatures of (A) fuel upflow nodes, (B) fuel downflow nodes, (C) fuel to fertile graphite nodes, and (D) fuel to fuel graphite nodes.

4. Reactor control strategy

For the purposes of this discussion, reactor control is considered distinctly from reactor safety features, which ensure safe shutdown of the reactor in the event of an anomalous condition that precludes continued operation of the plant. This discussion of reactor control is limited to the use of control systems to improve performance as compared with the open-loop, or uncontrolled, system. Ultimately, both deterministic and probabilistic safety analysis requires a complete engineering design of the plant. In this section, instrumentation for controller input purposes is discussed along with simulation of the controlled system response based upon simulation of these instrumentation approaches. Consideration is given to temperature sensor- and neutron detector-based control, in which thermodynamic power and neutron power, respectively, are compared with demand power at the ultimate heat sink, which is modeled as a simple power extraction value at the boiler and reheater.

4.1. MSR instrumentation and control

In discussing the instrumentation and control of any MSR system, it is prudent to consider the approaches used in the MSRE. The MSRE investigated the use of a servo motor-operated control rod in conjunction with thermocouples to measure the temperature of the fuel salt leaving the core [as measured by the temperature on the outside of the INOR-8 piping carrying fuel salt to the primary heat exchanger (INOR-8 is a nickel-based alloy that was developed at ORNL and is marketed under the brand name Hastelloy-N by

Haynes International)]. It was found that when changing the power level, minimal control action was taken via control rods due to the natural temperature feedback of the fuel salt and graphite moderator. When more heat was extracted at the ultimate heat sink for the MSRE, an air-cooled radiator, fuel salt temperature fell, increasing reactivity and raising the power level. Additionally, when lesser heat was extracted at the radiator, fuel salt temperature rose, decreasing reactivity and bringing the system to a lower power level.

Owing to the relatively long time it takes for a change in fuel salt temperature to be reflected in the temperature of the outside of the piping, natural feedback affected the necessary changes in reactor power before the temperature-based controller received information that the condition of the plant had changed. However, when the temperature set point of the system was changed by the operator, the servo system operating on the control rod succeeded in bringing the reactor to the new core exit temperature set point [10]. Similar behavior is observed in the MSBR system, and minimal external control action is required to operate the reactor.

The major challenges to MSRE instrumentation were due to the harsh environment presented by elevated temperatures, radiation, and chemical compatibility of the molten salt with detector materials. Multiple different salt compositions were studied, including using U-233 as the fissile material and varying the concentration of UF₄ in the fuel salt, but these changes did not affect the instrumentation and control design or implementation [11]. Similar challenges exist today, and research will be needed into developing new and improved instruments to better handle the harsh environment presented by all MSR systems.

4.2. Load following operation of the MSBR

The constant terms in the boiler and reheater equations are just fractional power removal terms representative of the power extracted by the boiler and reheater separately. These terms can be used as external inputs to change the heat extraction, therefore simulating changing power demand. Fig. 6 shows a plot of the reactivity feedback-induced response of the MSBR system to ramping down of demand power at a rate of 1%/min down to 50% of nominal power, and then subsequently increasing demand up to full power. The plot shows the demand power and fractional power as calculated from the neutron density, and the measured power. Apart from small transients seen at discontinuities in the demand power signal, the response of the reactor is stable and exhibits minor delay. The plot in Fig. 6B shows the response of the neutron power and measured power to change in demand power; notice the different ranges of the time axis. The time lag is of the order of ~10 seconds. This is approximately equal to the sum of the fuel salt and coolant salt circulation time. The power signal, as measured using thermocouples, is simulated using a first-order lag with a time constant of 5 seconds and a 1 second time delay. This simulates the time lag for heat transfer to a thermocouple placed outside INOR-8 piping. It must be mentioned that effects related to xenon-135 may influence the results shown here. Since no fission product removal is modeled, it is assumed that the plant operates a xenon removal system, like the one mentioned before, at a rate sufficient to counteract any significant buildup.

The spotlight here is particularly on the fact that the response of the reactor system shown in Fig. 6 is independent of any external

control action. The natural feedback of the MSBR system is sufficient to compensate for changes in power demand. The reactivity feedback responses are plotted in Fig. 7 corresponding to the plots in Fig. 6. In both Figs. 6B and 7B, the demand changes at $t = 500$ seconds. The reactivity feedback only starts to change after about $t \sim 508$ seconds, followed later by a change in the neutron power signal at about $t \sim 510$ seconds. The delay in feedback and the resulting fractional power are consequences of the circulating salts and the time taken for the temperature change in the final heat sink to be conveyed to the salts in the core. There are further delays due to the time needed to heat up the heterogeneous core. The measured signal, as mentioned before, is simulated. The reactor dynamics exhibits a self-regulation characteristic, without an explicit need for external reactivity perturbation for load following maneuvers.

Meanwhile, temperatures in the different nodes vary about an average as the demand power is varied. As mentioned earlier, the measured power depends only on the difference between the inlet and outlet temperatures (ΔT) of the fuel and fertile salt nodes. Thus, the temperature of the hottest leg of the reactor core decreases and the temperature of the coldest leg increases as the reactor power level follows the demand load. This is illustrated for the fuel node temperatures in Fig. 8. Also plotted is the fuel salt liquidus temperature, i.e., lowest temperature at which the fuel salt mixture is completely liquid. From a reactor safety point of view, this temperature marks a key violation. It is imperative that the various fuel salt-containing flow sections of the reactor be kept above this liquidus temperature during reactor operation. It is the same with other salt-containing parts of the system, although those liquidus temperatures vary depending on the salt mixture.

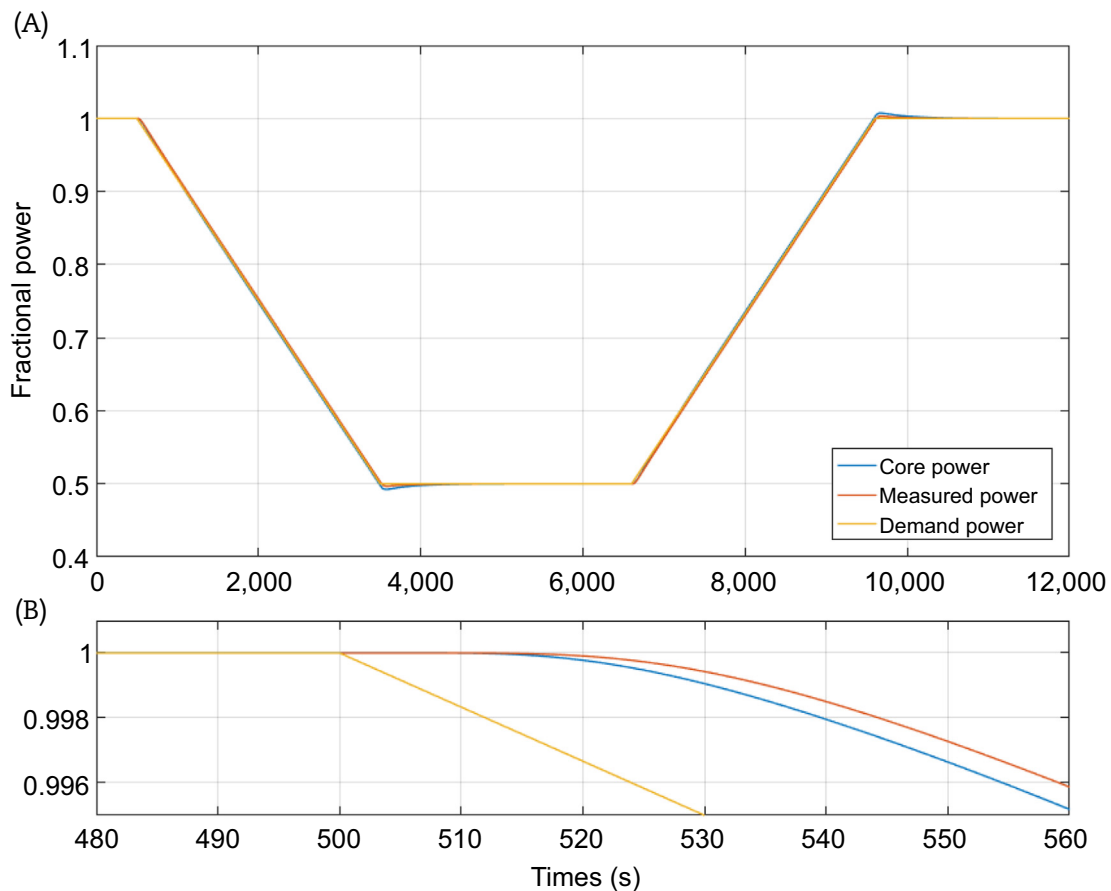


Fig. 6. Open-loop load following via temperature feedback reactivity (without controller). Core (neutronic) power, measured power (using thermocouples) and demand power for (A) load-following maneuver over time, and (B) enlarged view around $t = 500$ s showing response lag following change in demand power.

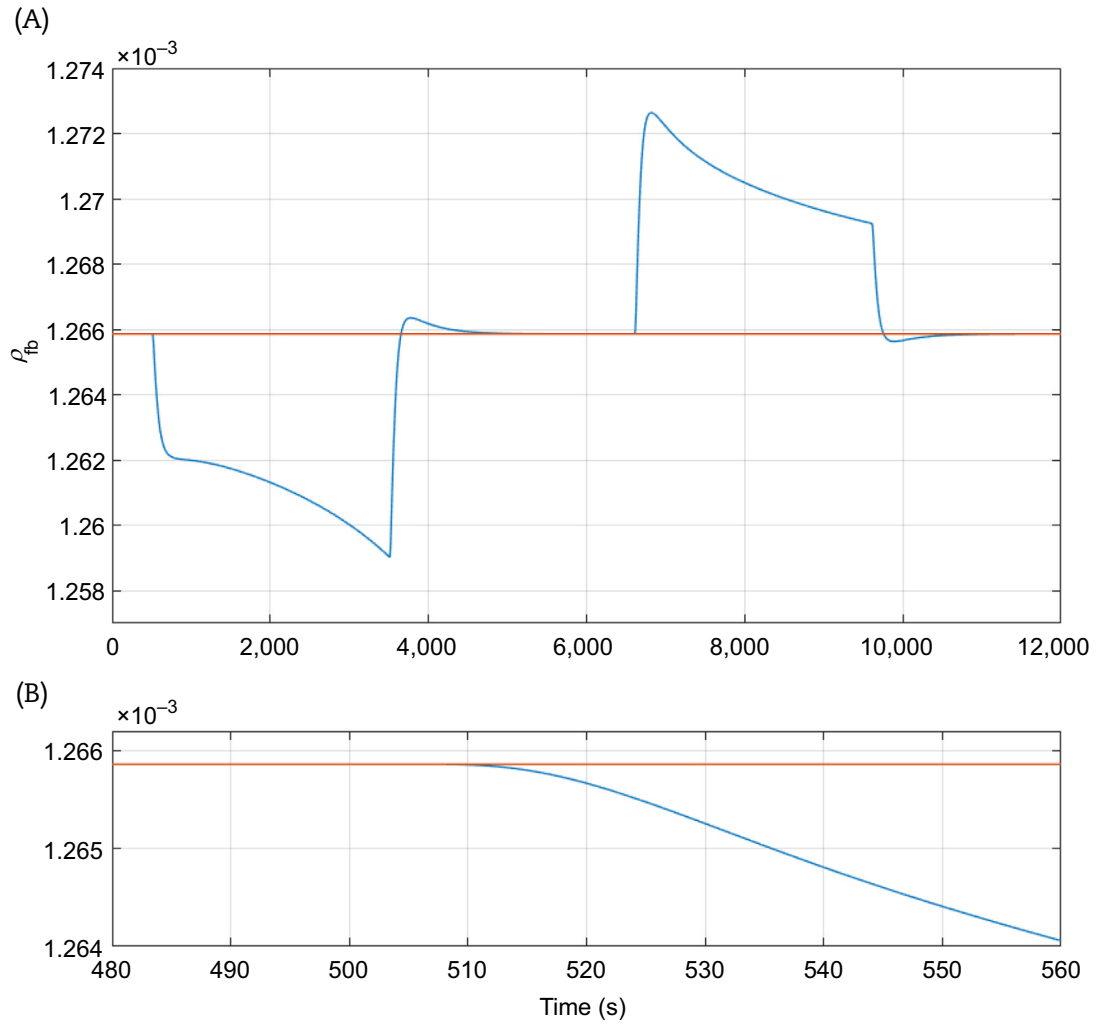


Fig. 7. Feedback reactivity response to change in demand power. Feedback reactivity for (A) load-following maneuver over time, and (B) enlarged view around $t = 500$ s showing lag in feedback response.

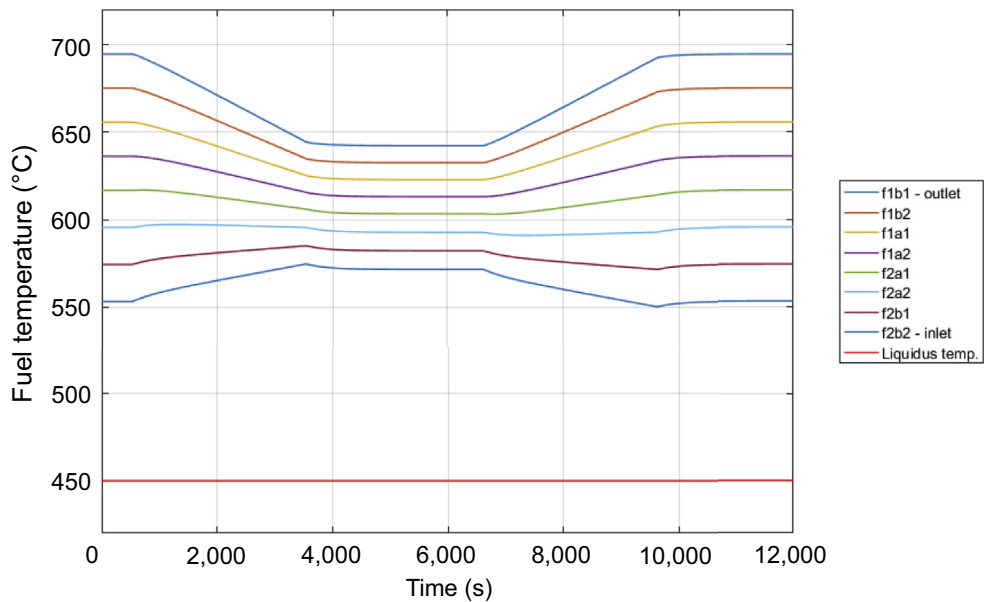


Fig. 8. Temperature response of core fuel nodes to change in demand power.

A closer examination of Fig. 8 suggests that the liquidus temperature can only be violated when the reactor power is ramped up at a very rapid rate. In this scenario, the coldest node temperature would decrease to below the liquidus temperature. In the case when the reactor power is zero, salts in the various nodes will converge to some temperature T_{avg} .

5. Concluding remarks

An enhanced nonlinear dynamic model for a two-fluid MSBR plant has been developed. The nodalized model accurately represents the reference design presented in the work of Robertson et al. [6]. A companion paper detailing the dynamic model of the MSBR is in preparation [8]. The model structure has been extended to the MSRE, and a companion paper comparing results of simulation with experimental data is also in preparation.

The simulation of dynamic response to reactivity perturbations illustrates the stability of the two-fluid model. Upon positive reactivity insertion, the model shows a prompt jump in power and the corresponding neutron density, as expected. The prompt jump is followed by an exponential fall to nominal power. Local peaks are seen on the otherwise smooth curve due to the introduction of delayed neutrons by the circulating fuel. Some higher-order peaks are also seen. A corresponding change in the feedback reactivity to compensate for the step insertion is also observed. Similar stability is observed in the case of periodic reactivity excursions.

A major observation is the open-loop load-following capability of the MSBR system to changes in demand power. The natural temperature feedback of the fuel salt and graphite (and to a smaller extent the fertile salt) to changes in power extraction at the ultimate heat sink seems to be sufficient to control the MSBR system. The resulting reactivity change compensates for the change in demand power and the reactor power is observed to change in a stable fashion. This self-regulation can be leveraged in well-designed MSBR systems to be used as on-demand and grid-stabilizing power generators in an economy that increasingly favors solar and wind, which are clean but intermittent power sources. Furthermore, temperatures in the salt-carrying sections of the plant are observed to be varying around an average. This means that the temperature of the hottest node decreases while the temperature of the coldest node increases during a load-following maneuver. Thus, salts in the various parts of the MSBR system do not freeze during load-following maneuvers leading to safe and stable operation. While these results are only accurate to a certain degree, it is remarkable that despite having a lower delayed

neutron fraction than pure U-235, and further losses in delayed neutrons due to circulation, the MSBR system still displays a high degree of stability. Even more impressive is the reactor's self-regulation in response to changes in demand power. This latter characteristic is an emergent behavior of the total feedback of this reactor system. It can be leveraged to engineer a truly “walk away” safe next-generation reactor.

Conflicts of interest

The authors declare that there is no conflict of interest.

Acknowledgments

The research and development reported in this paper is supported in part by a grant from Flibe Energy Inc., Huntsville, AL, with the University of Tennessee, and in part by the University of Tennessee Nuclear Engineering Enrichment Fund. The authors are grateful to Dr Tom Kerlin, Professor Emeritus of Nuclear Engineering, University of Tennessee, for the technical discussion about MSR.

References

- [1] L.E. McNeese, Molten-Salt Reactor Program semiannual progress report for period ending February 29, 1976, ORNL-5132, Oak Ridge National Laboratory, Oak Ridge (TN), 1976.
- [2] W.K. Ergen, A.D. Callihan, C.B. Mills, D. Scott, The aircraft reactor experiment—physics, *Nuclear Sci. Eng.* 2 (1957) 826–840.
- [3] P.N. Haubenreich, J.R. Engel, Experience with the Molten-Salt Reactor Experiment, *Nucl. Appl. Technol.* 8 (1970) 118–136.
- [4] R.C. Robertson, MSRE design and operations report part I: description of reactor design, ORNL-TM-0728, Oak Ridge National Laboratory, Oak Ridge (TN), 1965.
- [5] Documents Related to Liquid-Halide (Fluoride and Chloride) Reactor Research and Development [Internet], [cited 2016 Sep 9]. Available from: <http://www.energyfromthorium.com/pdf>.
- [6] R.C. Robertson, O.L. Smith, R.B. Briggs, E.S. Bettis, Two-fluid molten-salt breeder reactor design study, ORNL-4528, Oak Ridge National Laboratory, 1970.
- [7] J.R. Engel, R.C. Steffy Jr., Xenon behavior in the Molten-Salt Reactor Experiment, ORNL-TM-3464, Oak Ridge National Laboratory, Oak Ridge (TN), 1971.
- [8] T.W. Kerlin, Preliminary dynamics model of the MSBR, Intra-Laboratory Correspondence, MSR-67–102, Oak Ridge National Laboratory, Oak Ridge (TN), 1967.
- [9] H. Klee, R. Allen, *Simulation of Dynamic Systems with MATLAB and SIMULINK*, third ed., CRC Press, Boca Raton, 2011.
- [10] C.H. Gabbard, Performance of MSRE nuclear power control systems, ORNL-68-5-11, Oak Ridge National Laboratory, Oak Ridge (TN), 1968.
- [11] R.C. Steffy Jr., Experimental dynamic analysis of the MSRE with 233-U fuel, ORNL-TM-2997, Oak Ridge National Laboratory, Oak Ridge (TN), 1970, p. 23.